

Article

**Electrogenerated Chemiluminescence. 61. Near-IR Electrogenerated Chemiluminescence, Electrochemistry, and Spectroscopic Properties of a Heptamethine Cyanine Dye in MeCN**

Sang Kwon Lee, Mark M. Richter, Lucjan Strekowski, and Allen J. Bard

*Anal. Chem.*, 1997, 69 (20), 4126-4133 • DOI: 10.1021/ac9704570

Downloaded from <http://pubs.acs.org> on January 23, 2009

**More About This Article**

Additional resources and features associated with this article are available within the HTML version:

- Supporting Information
- Links to the 2 articles that cite this article, as of the time of this article download
- Access to high resolution figures
- Links to articles and content related to this article
- Copyright permission to reproduce figures and/or text from this article

[View the Full Text HTML](#)



**ACS Publications**  
High quality. High impact.

# Electrogenerated Chemiluminescence. 61. Near-IR Electrogenerated Chemiluminescence, Electrochemistry, and Spectroscopic Properties of a Heptamethine Cyanine Dye in MeCN

Sang Kwon Lee,<sup>†</sup> Mark M. Richter,<sup>†,§</sup> Lucjan Strekowski,<sup>‡</sup> and Allen J. Bard<sup>\*,†</sup>

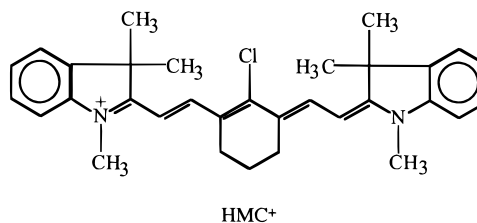
Department of Chemistry and Biochemistry, The University of Texas at Austin, Austin, Texas 78712, and Department of Chemistry, Georgia State University, Atlanta, Georgia 30303

**The oxidation of the heptamethine cyanine dye 2-[4'-chloro-7'-(1''-methyl-3'',3''-dimethylindolin-2''-ylidene)-3',5'-(propane-1''',3'''-diyl)-1',3',5'-heptatrien-1'-yl]-1-methyl-3,3-dimethylindolinium cation (HMC<sup>+</sup>) in the presence of tri-*n*-propylamine (TPrA) at +0.7 V vs SCE in MeCN produces near-IR electrogenerated chemiluminescence (ECL) with an emission maximum at about 805 nm and a relative ECL quantum efficiency of 0.21 vs Ru(bpy)<sub>3</sub><sup>2+</sup> (bpy = 2,2'-bipyridine) with TPrA in MeCN as a standard. The ECL emission spectra are identical to the photoluminescence spectra. The concentration dependence of the ECL is attributed to both self-absorption and competition by radical dimerization reactions. An oxidative-reduction mechanism for excited state formation is proposed and is compared to the Ru(bpy)<sub>3</sub><sup>2+</sup>/TPrA reference system. Digital simulation was employed to examine the kinetics of the homogeneous redox reaction between TPrA and HMC<sup>+</sup>. The rate constant for the catalytic reaction is >2000 M<sup>-1</sup> s<sup>-1</sup>, and the lower limit for proton transfer is 10<sup>7</sup> M<sup>-1</sup> s<sup>-1</sup>. Molecular mechanics calculations were used to determine the most stable configuration for the HMC<sup>+</sup> molecule.**

Electrogenerated chemiluminescence (ECL) involves the production of light at or near an electrode surface by energetic reactions involving electrogenerated species that result in the formation of excited states.<sup>1</sup> Many organic species, typically aromatic hydrocarbons and heterocycles, have been investigated as ECL-active species. The excited-state reaction typically involves an annihilation electron-transfer reaction between electrogenerated oxidized and reduced species (usually the radical ions) produced by cycling the electrode potential. In an alternative approach, excited states are generated with a potential step in one direction in the presence of a coreactant. For example, oxidation of an ECL-active species, R, in the presence of oxalate ion leads to emission via the reaction of R<sup>+</sup> and a reduced species (CO<sub>2</sub><sup>-</sup>) to produce

R\*.<sup>2</sup> ECL-active labels have been employed for sensitive and selective analytical methods, e.g., in immunoassay or DNA probes.<sup>3</sup> The reported ECL reactions typically yield emission in the visible region.<sup>4</sup> For analytical purposes, it is useful to have ECL labels that span a wide range of wavelengths so that simultaneous analysis of several analytes in a single sample is possible. We report here the first example of near-infrared ECL based on a heptamethine cyanine dye.

The heptamethine cyanine dye<sup>5</sup> used in this study was 2-[4'-chloro-7'-(1''-methyl-3'',3''-dimethylindolin-2''-ylidene)-3',5'-(propane-1''',3'''-diyl)-1',3',5'-heptatrien-1'-yl]-1-methyl-3,3-dimethylindolinium cation (HMC<sup>+</sup>). HMC<sup>+</sup> has two heterocyclic nuclei (3,3-



dimethylindole) linked by a conjugated carbon/carbon chain containing seven methine carbon atoms, a C–C trimethylene bridging group at the 10- and 12-methine positions, and alkyl groups at both nitrogen atoms, referred to as tricarbocyanine.

A molecular mechanics simulation of HMC<sup>+</sup> yields a structure (shown in the Supporting Information) in which the two 3,3-dialkylindole nuclei are distinctly coplanar, suggesting good delocalization and, hence, absorbance in the red–infrared (IR) region. The cyanine dyes, like HMC<sup>+</sup>, have been employed as

<sup>†</sup> University of Texas.<sup>‡</sup> Georgia State University.<sup>§</sup> Present address: Department of Chemistry, Southwest Missouri State University, Springfield, MO 65804.(1) (a) Faulkner, L. R.; Bard, A. J. In *Electroanalytical Chemistry*, Vol. 10; Bard, A. J., Ed.; Marcel Dekker: New York, 1977. (b) Faulkner, L. R.; Glass, R. S. In *Chemical and Biological Generation of Excited States*; Adam, W., Cilento, G., Eds.; Academic Press: New York, 1982. (c) Knight, A. W.; Greenway, G. M. *Analyst* **1994**, *119*, 879.(2) (a) Rubinstein, I.; Bard, A. J. *J. Am. Chem. Soc.* **1981**, *103*, 512. (b) Chang, M.-M.; Saji, T.; Bard, A. J. *J. Am. Chem. Soc.* **1977**, *99*, 5399. (c) Rubinstein, I.; Martin, C. R.; Bard, A. J. *Anal. Chem.* **1983**, *55*, 1580. (d) Ege, D.; Becker, W. G.; Bard, A. J. *Anal. Chem.* **1984**, *56*, 2413.  
(3) (a) Bard, A. J.; Whitesides, G. M. U.S. Patents 5 221 605, 1993; 5 238 808, 1993; and 5 310 687, 1994. (b) Blackburn, G. F.; Shah, H. P.; Kenien, J. H.; Leland, J.; Kamin, R. A.; Link, J.; Peterman, J.; Powell, M. J.; Shah, A.; Talley, D. B.; Tyagi, S. K.; Wilkins, E.; Wu, T.-G.; Massey, R. J. *J. Clin. Chem.* **1991**, *37*, 1534.  
(4) (a) Debad, J. D.; Lee, S. K.; Qiao, X.; Pascal, R. A., Jr.; Bard, A. J. *Acta Chem. Scand.*, in press. (b) Keszthelyi, C. P.; Tachikawa, H.; Bard, A. J. *J. Am. Chem. Soc.* **1973**, *94*, 1552. (c) Keszthelyi, C. P.; Tokel-Takvoryan, N. E.; Bard, A. J. *Anal. Chem.* **1975**, *47*, 249. (d) Richards, T. C.; Bard, A. J. *Anal. Chem.* **1995**, *67*, 3140.  
(5) (a) Strekowski, L.; Lipowska, M.; Patonay, G. *Synth. Commun.* **1992**, *22*, 2593. (b) Strekowski, L.; Lipowska, M.; Patonay, G. *J. Org. Chem.* **1992**, *57*, 4578.

the light-absorbing media in optical recording systems and as laser dyes because of their high molar absorptivity ( $\sim 2 \times 10^5 \text{ M}^{-1} \text{ cm}^{-1}$ ), absorption bands in the red–near-IR region (650–1000 nm), long-wavelength emission, and large Stokes shift.<sup>6</sup> They have also been employed as fluorescent probes in analysis, since their long-wavelength emission is outside the range for the emission of most biomolecules of interest.<sup>7,8</sup>

We describe here the electrochemistry of  $\text{HMC}^+$  and relate it to previous studies of the electrochemical oxidation of cyanine dyes.<sup>9,10</sup> We show that oxidation of  $\text{HMC}^+$  in the presence of tri-*n*-propylamine (TPrA) in MeCN solution produces ECL and discuss the mechanism of both the electrochemical and ECL reactions.

## EXPERIMENTAL SECTION

**Chemicals.** MeCN (UV grade, Burdick and Jackson, Baxter Health Care Corp., Muskegon, MI), silver tetrafluoroborate (98%, Aldrich, Milwaukee, WI), tri-*n*-propylamine (TPrA, 98%, Aldrich), and IR-125 ( $\text{C}_{43}\text{H}_{47}\text{N}_2\text{NaO}_6\text{S}_2$ , laser grade, Acros Organics, Pittsburgh, PA) were used as received. All UV/visible, fluorescence, electrochemical, and ECL solutions were prepared in a glovebox (Vacuum Atmospheres Corp., Los Angeles, CA) under a helium atmosphere and sealed in air-tight cells. Tetra-*n*-butylammonium hexafluorophosphate ((TBA)PF<sub>6</sub>, SACHEM, Inc., Austin, TX) was recrystallized from ethanol/water (4:1 v/v) three times, dried in vacuo at 100 °C, and stored in a glovebox before use. Ru(bpy)<sub>3</sub>(ClO<sub>4</sub>)<sub>2</sub> was prepared from the dichloride salt.<sup>11</sup>

The heptamethine cyanine dye,  $\text{HMC}^+\text{I}^-$ , was available from previous studies.<sup>5</sup> It was converted to the tetrafluoroborate salt via metathesis with AgBF<sub>4</sub>. Special care was taken to remove excess Ag<sup>+</sup> by thorough washing with deionized water. The sample was dried in vacuo at 50 °C for 15 h. Deionized water from a Millipore Milli-Q system was used throughout.

**Apparatus and Procedures.** Cyclic voltammograms with simultaneous photon detection were recorded using a Princeton Applied Research Model 173/175 potentiostat/universal programmer (PAR, Princeton, NJ) in conjunction with a Hamamatsu C1230 photon counter (Bridgewater, NJ) equipped with a Hamamatsu R928-P photomultiplier tube. The photomultiplier tube was housed in a water-jacketed Products For Research, Inc. Model TE308TSRF refrigerated chamber maintained at –10 °C. For plots of ECL intensity vs potential, the output from the photon counter was fed into the y-axis of the an Omnigraphic 2000 x–y recorder (Bausch and Lomb-Houston Instrument Division, Austin, TX).

A charge-coupled device (CCD) camera (Photometrics CH260), cooled to below –125 °C and interfaced to a PC, was used to obtain

ECL spectra. The camera was focused on the output of a grating spectrometer (Holographics, Inc., 1 mm entrance slit). The CCD camera and general configuration of the spectra acquisition have been described previously.<sup>12</sup> The relative efficiency of the ECL process in the  $\text{HMC}^+$ /TPrA system was determined by comparing the photons of light produced per Coulomb passed vs Ru(bpy)<sub>3</sub><sup>2+</sup> annihilation with TPrA in MeCN as a standard. ECL spectra were corrected for the wavelength dependence of the spectral distribution of the CCD after subtraction of background emission.

Cyclic voltammetry and bulk electrolysis experiments utilized either a Model 660 electrochemical workstation (CH Instruments, Memphis, TN) or the PAR 173/175. Electrochemical and ECL experiments utilized a conventional three-electrode cell configuration. The working electrode consisted of an inlaid platinum disk (1.5 or 2.1 mm diameter) that was polished on a felt pad with 0.05 μm alumina (Buehler) and sonicated in absolute EtOH for 1 min before each experiment. A platinum wire served as the counter electrode. Platinum gauze electrodes were used as working and counter electrodes in all bulk electrolysis experiments. A silver wire served as a quasi-reference electrode and was referenced to a Ag/Ag<sup>+</sup> electrode (Ag/AgBF<sub>4</sub>) in MeCN for the determination of redox potentials. All potentials are reported vs an aqueous saturated calomel electrode (SCE) obtained by addition of the potential difference (+0.28 V) between a Ag/AgBF<sub>4</sub> electrode in MeCN and an aqueous SCE.

UV/visible spectra were acquired on a Milton Roy Spectronic 3000 array spectrophotometer. Fluorescence spectra were obtained using an SLM Aminco SPF-500 spectrofluorometer. The spectra were measured by the front-surface method to avoid self-absorption and were excited at a wavelength of 774 nm. The fluorescence quantum yields were calculated<sup>13</sup> relative to IR-125 as a secondary standard ( $\phi_f = 0.13$  in DMSO,<sup>14</sup> excitation at 765 nm and fluorescence emission at 835 nm) using the following formula:

$$\phi_f = \phi_{f,s} \left( \frac{F}{F_s} \right) \left( \frac{\epsilon_s}{\epsilon} \right) \left( \frac{E_s}{E} \right) \left( \frac{n^2}{n_s^2} \right) \quad (1)$$

where  $F$  is the integrated area under the fluorescence emission profile,  $\epsilon$  is the molar absorptivity of  $\text{HMC}^+$  at the excitation wavelength,  $E$  is the intensity of the excitation light,  $n$  is the refractive index of the solvent, and the subscript s designates those parameters associated with the standard.

Digital simulations for electrochemical oxidation of TPrA with  $\text{HMC}^+$  were run on a PC using DigiSim (BAS, West Lafayette, IN).

## RESULTS AND DISCUSSION

**Electrochemistry of  $\text{HMC}^+$ .** Figure 1 shows typical cyclic voltammograms for the oxidation of 1 mM  $\text{HMC}^+$  (MeCN/0.1 M (TBA)PF<sub>6</sub>) at a scan rate,  $v$ , of 0.2 V/s. The one-electron oxidation of  $\text{HMC}^+$  generates the corresponding radical dication at +0.55 V vs SCE. The wave is both chemically and electrochemically reversible at this scan rate. At much slower scan rates (<0.02 V/s), however, the oxidation wave becomes slightly irreversible, suggesting that the radical dication undergoes slow decomposi-

- (6) (a) Patonay, G.; Antoine M. D. *Anal. Chem.* **1991**, *63*, 321A. (b) Matsuoka, M., Ed. *Infrared Absorbing Dyes*; Plenum Press: New York, 1990. (c) Waring, D. R., Hallas, G., Eds. *The Chemistry and Applications of Dyes*; Plenum Press: New York, 1990.
- (7) Williams, R. J.; Narayanan, N.; Casay, G. A.; Lipowska, M.; Strekowski, L.; Patonay, G.; Peralta, J. M.; Tsang, V. C. W. *Anal. Chem.* **1994**, *66*, 3102.
- (8) (a) Zen, J.; Patonay, G. *Anal. Chem.* **1991**, *63*, 2934. (b) Patonay, G.; Antoine M. D.; Devanathan, S.; Strekowski, L. *Appl. Spectrosc.* **1991**, *45*, 457. (c) Williams, R. J.; Lipowska, M.; Patonay, G.; Strekowski, L. *Anal. Chem.* **1993**, *65*, 601. (d) Netzel, T. L.; Nafisi, K.; Zhao, M.; Lenhard, J. R.; Johnson, I. J. *Phys. Chem.* **1995**, *99*, 17936. (e) Shealy, D. B.; Lipowska, M.; Lipowski, J.; Narayanan, N.; Sutter, S.; Strekowski, L.; Patonay, G. *Anal. Chem.* **1995**, *67*, 247.
- (9) Lenhard, J. R.; Cameron, A. D. *J. Phys. Chem.* **1993**, *97*, 4916.
- (10) (a) Lenhard, J. R.; Parton, R. L. *J. Am. Chem. Soc.* **1987**, *109*, 5808. (b) Parton, R. L.; Lenhard, J. R. *J. Org. Chem.* **1990**, *55*, 49.
- (11) Tokel-Takvoryan, N. E.; Hemingway, R. E.; Bard, A. J. *J. Am. Chem. Soc.* **1973**, *95*, 6582.

- (12) McCord, P.; Bard, A. J. *J. Electroanal. Chem.* **1991**, *318*, 91.
- (13) (a) Morris, J. V.; Mahaney, M. A.; Huber, R.; Demas, J. J. *Phys. Chem.* **1976**, *80*, 969–974. (b) Crosby, G. *J. Phys. Chem.* **1971**, *75*, 991–1024.
- (14) Benson, R. C.; Kues, H. *J. Chem. Eng. Data* **1977**, *22*, 379–383.

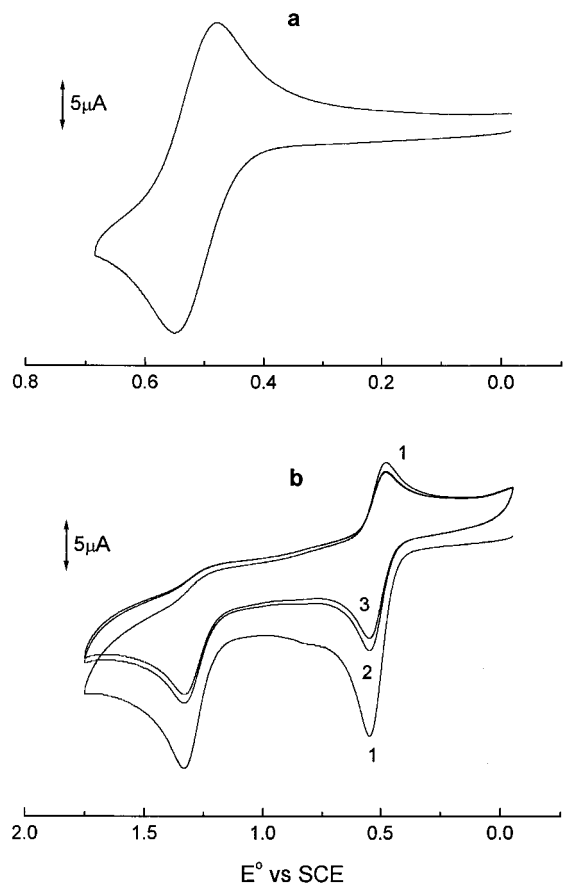


Figure 1. Cyclic voltammograms of 1.0 mM HMC<sup>+</sup> in MeCN; scan rate, 0.2 V/s. (a) Single scan and (b) multiple scans with the oxidation of HMC<sup>2+</sup> (1 = first scan). Electrolyte, 0.1 M (TBA)PF<sub>6</sub>.

tion, probably via a dimerization reaction.<sup>9,10</sup> For di- and tricyanine dyes, the reversibility of the cyclic voltammograms in MeCN depends on the nature of substitution within the polymethine chain. For example,<sup>10a</sup> an unsubstituted thiadicarbocyanine dye undergoes an irreversible process at scan rates of 0.02–2.0 V/s. At higher scan rates, the dimerization reaction can be partially outrun, and a quasireversible wave is observed. On the other hand, thiadicarbocyanine dyes containing substituents within the pentamethine chain, which electronically stabilize the radical dication and sterically inhibit dimerization, exhibit reversible cyclic voltammetry.<sup>10</sup> In HMC<sup>+</sup>, the addition of the C–C trimethylene bridging group at the 10- and 12-methine positions and alkyl groups at both nitrogen atoms of the heptamethine cyanine dye enhances the stability of the tricyanine radical dication and the steric hindrance and produces the reversible voltammogram shown in Figure 1a. The substitutions also result in a decrease of the one-electron potential for oxidation, although it is difficult to compare accurately these factors because of differences of heterocyclic nuclei.

HMC<sup>+</sup> undergoes a second, chemically irreversible oxidation at +1.33 V vs SCE (Figure 1b). This agrees with the work of Lenhard and Cameron, who investigated a series of cyanine dyes<sup>9</sup> and found in all cases a chemically irreversible second anodic wave, corresponding to the one-electron oxidation of the radical dication to the trication. The oxidation peak current of wave 1 of the first scan in Figure 1b is the same as that in Figure 1a. However, the instability of the trication produced in the second oxidation wave leads to a reduction in the peak current of wave 1 in scan 1 in Figure 1b which is less than half of that in Figure 1a.

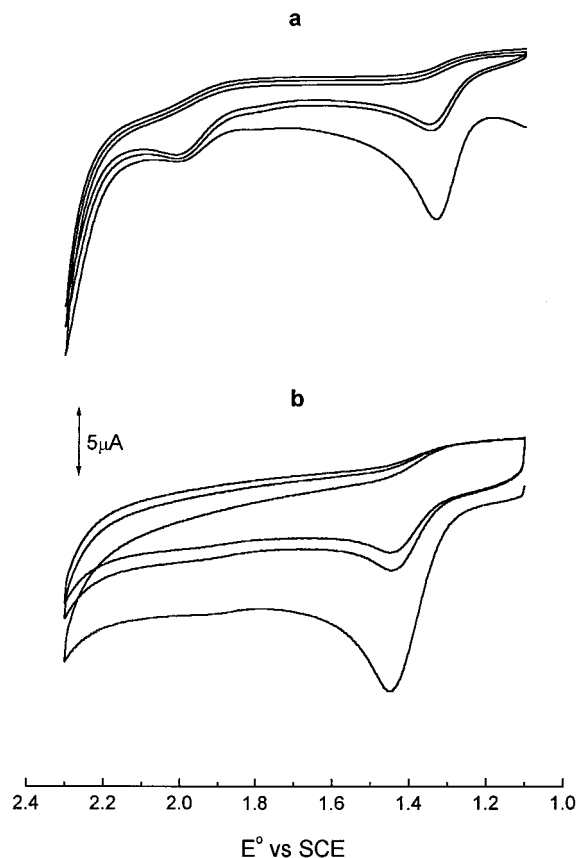


Figure 2. Cyclic voltammograms of 1.0 mM HMC<sup>+</sup> in MeCN, scan rates (a) 0.05 and (b) 5 V/s. Electrolyte, 0.1 M (TBA)PF<sub>6</sub>.

Sequential scans result in essentially steady-state behavior within 2–3 scans. The current–potential response on scanning from 0 to 0.7 V was linear with  $v^{1/2}$ , from 0.02 to 100 V/s, indicating that the electrochemical reactions are diffusion-controlled.

Cyanine radical dications are susceptible to radical–radical dimerization at the even-methine carbon atoms of the polymethine chain;<sup>10</sup> hence, methine chain substituents would be expected to impart both steric and electronic effects that influence radical reactivity. Cyclic voltammetry of 1 mM HMC<sup>+</sup> was carried out by scanning the potential from +1.1 to +2.3 V at several sweep rates and concentrations. Figure 2 shows representative cyclic voltammograms at scan rates of 0.05 (Figure 2a) and 5.0 V/s (Figure 2b). Two waves were observed at  $v = 0.05$  V/s (Figure 2a), one at +1.3 V, corresponding to dication–trication oxidation, and the second at +2.0 V, probably characteristic of the product of the dimerization reaction. The peak current of this wave increased with sequential scans and showed an inverse dependence on  $v$ . With 1 mM HMC<sup>+</sup>, the third oxidation wave was not seen at scan rates greater than 5.0 V/s (Figure 2b), but at 5 mM HMC<sup>+</sup>, it was present up to 100 V/s. At lower concentrations (<0.1 mM), the third oxidation peak was not found, even at very slow scan rates. This is consistent with dication dimerization. The addition of substituents within the methine chain of HMC<sup>+</sup> tends to stabilize the dications with respect to dimerization by steric effects and electronic stabilization.

Several cathodic voltammetric waves were observed. Waves probably characteristic of carbon–chloride bond reduction and a quasi-reversible wave for HMC<sup>+</sup> reduction appeared at –1.74 and –0.73 V vs SCE, respectively. Neutral radicals for most cyanine dyes are generally more reactive than their radical dication

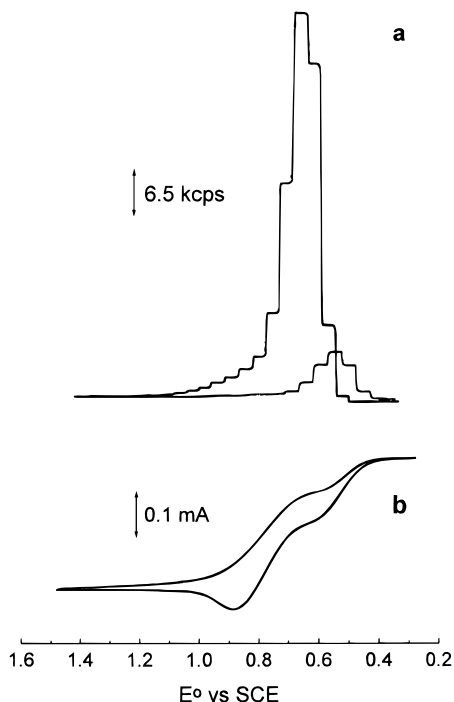


Figure 3. (a) ECL emission-potential transient and (b) cyclic voltammogram of  $2.0 \times 10^{-4}$  M HMC<sup>+</sup> and 0.06 M TPrA in MeCN. Scan rate, 0.05 V/s; electrolyte, 0.1 M (TBA)PF<sub>6</sub>. The staircase shape of the emission is the result of integration of the photon flux in the single-photon-counting system (cps = photomultiplier counts per second).

counterparts.<sup>9</sup> The instability of the reduced form of HMC<sup>+</sup> prevents efficient generation of ECL via annihilation of HMC<sup>•</sup> and HMC<sup>2+</sup>. However, the good stability of HMC<sup>2+</sup> suggested that oxidation in the presence of a coreactant could produce ECL.

**Electrogenerated Chemiluminescence.** The cyclic voltammetry and ECL for 0.2 mM HMC<sup>+</sup> with 0.06 M TPrA as coreactant (MeCN/0.1 M (TBA)PF<sub>6</sub>) during a potential sweep from -0.2 to +1.7 V ( $v = 0.05$  V/s) are shown in Figure 3. The broad, irreversible wave at about +1.1 V (Figure 3b) is due to the direct oxidation of TPrA at the electrode. The HMC<sup>+</sup> oxidation wave, barely seen in this scan because of its low relative concentration, is enhanced about 10-fold by the presence of TPrA (compared to a solution of 0.2 mM HMC<sup>+</sup> alone), and the corresponding cathodic wave is lost, signaling, as discussed later, a catalytic reaction between the dication and TPrA. The ECL appears in Figure 3a at the potential for the HMC<sup>+</sup> oxidation wave, suggesting that the catalytic reaction is the source of the ECL. No emission is observed in the absence of either TPrA or HMC<sup>+</sup>. On the forward scan, the emission intensity rises as the catalytic current increases. On the reverse scan, the intensity and current are smaller. The maximum ECL emission occurred at +0.68 V, 130 mV more positive than the potential for oxidation of HMC<sup>+</sup> (+0.55 V). Although the potential for the peak ECL emission is in the range where TPrA oxidation starts, the intensity of the ECL emission increased with the concentration of HMC<sup>+</sup> at constant TPrA concentration.

The ECL emission was not visible, even to the dark-adapted eye, because it occurred in the near-IR region. It could, however, be imaged with the CCD camera by focusing the camera on the electrode/solution (0.05 mM HMC<sup>+</sup>/0.4 M TPrA) interface with the potential repeatedly stepped from 0 to +1.0 V (pulse width,

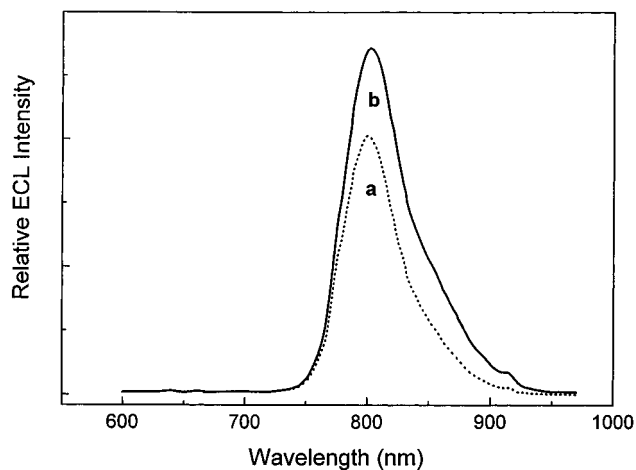


Figure 4. ECL spectrum, (a) uncorrected and (b) corrected, of  $2.0 \times 10^{-4}$  M HMC<sup>+</sup> with 0.06 M TPrA in MeCN. The potential was stepped from 0 to 1.4 V, and the exposure time was 5 min. Electrolyte, 0.1 M (TBA)PF<sub>6</sub>.

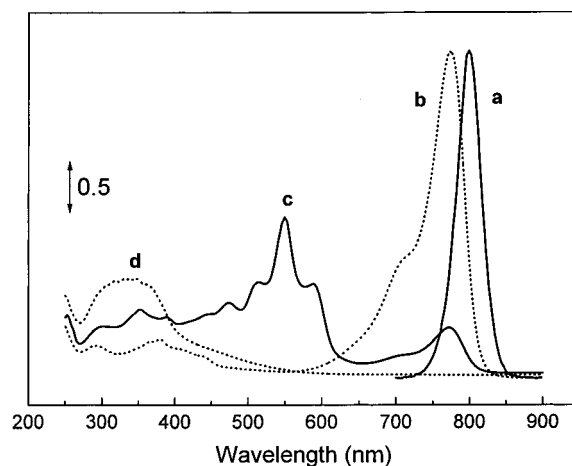
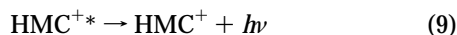
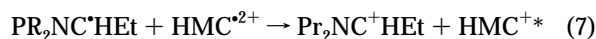
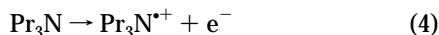
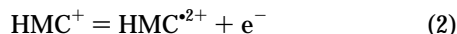


Figure 5. (a) Fluorescence spectrum of  $1.0 \times 10^{-5}$  M HMC<sup>+</sup> ( $\lambda_{\text{ex}} = 774$  nm) and absorption spectra obtained (b) before and (c) after controlled potential bulk electrolysis at 0.7 V. (d) Exhaustive electrolysis at 0.7 V for 10 h of  $1.0 \times 10^{-4}$  M HMC<sup>+</sup> in MeCN.

0.2 s; exposure time, 15 min). The observed emission intensity at the platinum electrode suggested a high ECL efficiency. Figure 4 shows both corrected and uncorrected ECL spectra for HMC<sup>+</sup>/TPrA. The ECL spectrum of Figure 4b was corrected for wavelength response of the CCD camera, as described in the Experimental Section. The emission spectra were centered around 805 nm, slightly shifted to lower wavelengths from the fluorescence (Figure 5a) due to an inner-filter effect. Because the ECL solution is more concentrated than the solution used for the fluorescence measurement, the shorter wavelengths are absorbed upon passage through the HMC<sup>+</sup> solution. A comparison of the ECL and fluorescence spectra (Figures 4 and 5a, respectively) shows that they are similar in shape and energy, suggesting that emission is from the same excited singlet state of HMC<sup>+</sup>. The relative ECL efficiency ( $\phi_{\text{ECL}}$ , compared to Ru(bpy)<sub>3</sub><sup>2+</sup>/TPrA at the same concentration) was 0.21 for the HMC<sup>+</sup>/TPrA system using values from the corrected spectrum ([HMC<sup>+</sup>] = 0.2 mM and [TPrA] =  $6.0 \times 10^{-2}$  M).

The mechanism of the ECL reaction probably follows similar reactions involving an ECL-active molecule and the coreactant TPrA. This coreactant was introduced by Noffsinger and Daniel-

son<sup>15</sup> and the mode of reaction studied by Leland and Powell.<sup>16</sup> Although firm evidence for the intermediates and reaction kinetics is still needed, the overall mechanism, in which a strong reductant, Pr<sub>2</sub>NCHet, is produced upon oxidation of TPrA, follows the general ECL reaction scheme, where the excited state is produced by an electron-transfer reaction:



Reactions 2 and 3 constitute the catalytic reaction sequence that affects the magnitude of the first oxidation wave of HMC<sup>+</sup> in the presence of Pr<sub>3</sub>N. We examine the details of the catalytic reaction by digital simulation below.

**Absorption Spectra.** To obtain information about the stability of HMC<sup>2+</sup>, absorbance spectra were obtained during the bulk electrolytic oxidation of HMC<sup>+</sup>. Figure 5b–d shows the absorption spectra for a 0.01 mM solution of HMC<sup>+</sup> in MeCN obtained before (b) and after (c) exhaustive one-electron oxidation at +0.7 V. The current was monitored throughout the experiment. At higher concentrations (e.g., 1 mM), color changes attributable to different electrogenerated species were observed, proceeding sequentially from green to blue to purple to red. HMC<sup>+</sup> itself exhibits a low-energy absorption maximum at 774 nm (green) and a molar extinction coefficient ( $\epsilon$ ) of  $2.41 \times 10^5 \text{ M}^{-1} \text{ cm}^{-1}$ , characteristic of cyanine dyes.<sup>9,10,17</sup> The controlled potential bulk electrolysis at +0.7 V almost immediately (<30 s) produced a deep blue-colored species, the radical dication. This species was unstable over a long time period, with regeneration of HMC<sup>+</sup> (green) on standing after about 1 h. Oxidation for longer times produced purple- and red-colored species that were generally stable and which exhibited absorption spectra typical of radical dications (Figure 5c).<sup>10</sup> However, regeneration of HMC<sup>+</sup> on standing was observed from the purple species after about 2 days. As the oxidation progressed from green through red, the low-energy absorption at 774 nm decreased in intensity, and peaks characteristic of the radical dication appeared at 555 nm. The principal absorption band for the radical dication is blue-shifted (about 220 nm) relative to the main band of the parent chromophore, and the molar extinction coefficient for this band is approximately half ( $1.21 \times 10^5 \text{ M}^{-1} \text{ cm}^{-1}$ ) that observed for the parent dye molecule. Similar results were observed by Lenhard and Cameron.<sup>9</sup> The basic shape of the lowest-energy absorption band of the radical dication closely resembles that of the parent

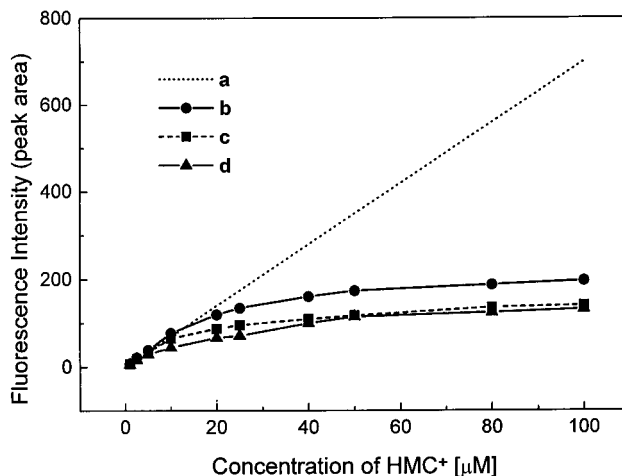


Figure 6. Effect of HMC<sup>+</sup> concentration on the fluorescence peak area in MeCN. The fluorescence spectrum was obtained by front-surface illumination. (a) Extrapolated low-concentration region. Emission measured at angles of (b) 80°, (c) 90°, and (d) 102° relative to excitation beam.

dye, except for a small shift (100–200 cm<sup>-1</sup>) in the position of the vibronic shoulder. This similarity in spectral bandshapes supports the conclusion that there are no gross differences in the overall structure (bond lengths, molecular conformation, etc.) between dye and radical dication.

The absorption spectrum obtained after exhaustive electrooxidation of 0.2 mM HMC<sup>+</sup> is shown in Figure 5d. The solution ultimately turned yellow, with no return with time to the initial green solution typical of dimerization of radical dications.<sup>10a</sup> Dimers were readily generated when a potential of  $\geq +2.0 \text{ V}$  was applied, signaling rapid dimerization of the 3+ species. In the potential region used in the ECL experiments, however, dimerization was slow.

**Fluorescence Spectra.** The fluorescence spectrum for 0.01 mM HMC<sup>+</sup> in MeCN (Figure 5a) occurs in the near-IR region centered around 800 nm ( $\lambda_{\text{ex}} = 774 \text{ nm}$ ). The absorption spectrum shown in Figure 5b emphasizes the small Stokes shift of 24 nm. This follows from the fact that the 0 → 0 vibrational bands in the absorption and emission spectra overlap,<sup>18</sup> leading to reabsorption or self-absorption of the emitted light in the overlap region at higher concentrations. This is a disadvantage in applications directly related to ECL. To avoid self-absorption effects, the fluorescence spectrum was obtained by the front-surface method, which records fluorescence at a nearly 90° angle chosen to minimize specular reflectance.<sup>18</sup> A plot of the peak area of the fluorescence vs concentration is shown in Figure 6 for HMC<sup>+</sup> in MeCN. The peak area of the emitted light was linear up to 0.05 mM HMC<sup>+</sup>. At higher concentrations, however, the linearity disappeared, even with the front-surface method. This indicates that a concentration-dependent process other than self-absorption is competing with fluorescence to deactivate the HMC<sup>+</sup> singlet state. If dimers of HMC<sup>+</sup> are produced upon irradiation, this suggests that the dimerization may occur from the excited state. Photoinduced quenching effects have been observed for a water-soluble heptamethine dye when it was excited with a semiconductor laser and were attributed to a dimerization process.<sup>7</sup> The fluorescence efficiency ( $\phi_{\text{fl}}$ ) of HMC<sup>+</sup> is 0.11 ( $\lambda_{\text{em}} = 800 \text{ nm}$ ,  $\lambda_{\text{exc}}$

(15) Noffsinger, J. B.; Danielson, N. D. *Anal. Chem.* **1987**, *59*, 865.

(16) Leland, J. K.; Powell, M. J. *J. Electrochem. Soc.* **1990**, *137*, 3127.

(17) Fabian, J.; Hartmann, H. *Light Absorption of Organic Colorants*; Springer-Verlag: Berlin, 1980.

(18) Cowan, D. O.; Drisko, R. L. *Elements of Organic Photochemistry*; Plenum Press: New York, 1976.

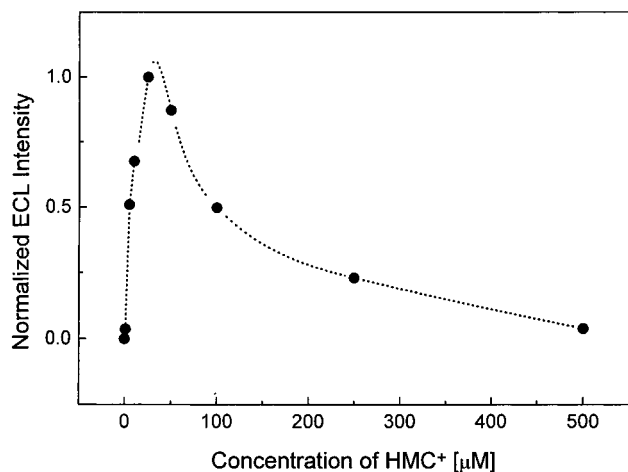


Figure 7. Effect of HMC<sup>+</sup> concentrations on the ECL intensity at  $4.0 \times 10^{-2}$  M TPrA in MeCN. Electrolyte, 0.1 M (TBA)PF<sub>6</sub>.

= 774 nm), as measured by the front-surface method in MeCN with IR-125 as a secondary standard ( $\phi_n = 0.13$ ).<sup>14</sup>

**Concentration Dependence of ECL Emission.** The ECL intensity increased with increasing TPrA concentration, up to 0.5 M (the solubility limit of TPrA in MeCN) at constant HMC<sup>+</sup> concentration. In a cyclic voltammogram containing high concentrations (0.05–0.1 M) of TPrA and HMC<sup>+</sup>, the peak height of the oxidation wave was proportional to TPrA concentration. HMC<sup>+</sup>, however, is unstable in TPrA solution and decomposes within a short time (within minutes). The rate of decomposition was faster at high concentrations of TPrA (>0.1 M) and with low concentrations of HMC<sup>+</sup> (<0.1 mM).

We also investigated the relationship between ECL intensity and HMC<sup>+</sup> concentration. In these experiments, the platinum electrode was immersed in solutions of different concentrations of HMC<sup>+</sup> at constant TPrA concentration (0.04 M), and the ECL emission was recorded during a potential sweep from 0 to +1.7 V at a scan rate of 0.05 V/s. The ECL peak emission was normalized with respect to the largest emission observed within a series of concentrations after subtraction of background emission. Figure 7 shows a plot of the normalized ECL emission vs the HMC<sup>+</sup> concentration. The observed response is roughly consistent with the results of the fluorescence experiments, with the ECL emission increasing with HMC<sup>+</sup> concentration up to 25 μM. At higher concentrations, the ECL emission intensity decreased with increasing HMC<sup>+</sup> concentration, suggesting that, as in the fluorescence studies, the radical cations undergo radical dimerization reactions as well as self-absorption.

**Digital Simulation for the Mechanism of the Electrochemical Oxidation of HMC<sup>+</sup> with TPrA.** Although the overall mechanism of the reaction involving the oxidation of HMC<sup>+</sup> and TPrA is complicated, the cyclic voltammetry should be largely governed by the catalytic sequence involving reactions 2 and 3. A study of the effect of scan rate,  $v$ , and TPrA concentration on the oxidation of HMC<sup>+</sup> should provide an estimate for the rate constant for reaction 3. This study was carried out by comparing experimental cyclic voltammograms of the first wave with those obtained by digital simulation using the commercial package Digisim (Figures 8 and 9). At large  $v$ , e.g., 20 V/s (Figure 8d), the rate of reaction 3 was too slow to perturb the concentrations of HMC<sup>+</sup> and HMC<sup>2+</sup> near the electrode, so the voltammogram is essentially that for the reversible oxidation of HMC<sup>+</sup>. With

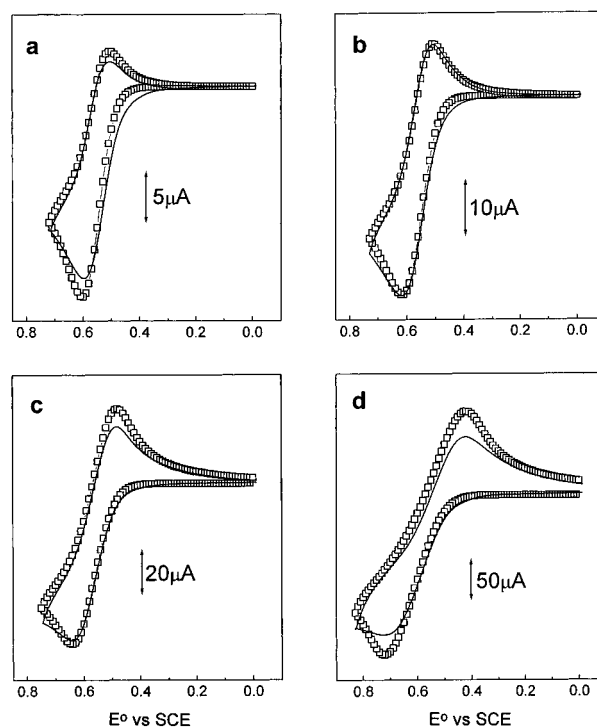


Figure 8. Effect of scan rate on cyclic voltammograms by the experimental (solid lines) and digital simulations (open circles) of 2.1 mM HMC<sup>+</sup> with 1.9 mM TPrA in MeCN; electrolyte, 0.1 M (TBA)PF<sub>6</sub>. (a) 0.05, (b) 0.2, (c) 2, and (d) 50 V/s at a 2.0 mm diameter Pt electrode. Background was subtracted from the experimental data. Simulation parameters: eq 2,  $E^\circ = +0.55$  V vs SCE,  $\alpha = 0.5$ ,  $k_s = 1.8 \times 10^{-2}$  cm/s; eq 3,  $k_f$  (the forward rate) = (a) 2000, (b) 2500, (c) 2000, and (d) 2500 M<sup>-1</sup> s<sup>-1</sup>; eq 5,  $k_f = 1.5\text{--}5 \times 10^7$  M<sup>-1</sup> s<sup>-1</sup>; eq 8,  $k_f = 41$  s<sup>-1</sup>.

sweeps to more positive potentials, it is followed by the direct irreversible oxidation of TPrA, reaction 4. When the scan rate is decreased, the rate of reaction 3 becomes significant, leading to regeneration of HMC<sup>+</sup> at potentials of the first wave. This causes the anodic wave for HMC<sup>+</sup> oxidation to increase and the reversal cathodic wave for HMC<sup>2+</sup> reduction to decrease (Figure 8a,b). Consumption of TPrA at potentials of the first wave also causes a decrease in the anodic peak current for its direct oxidation. When the TPrA concentration is higher than that of HMC<sup>+</sup> (Figure 9b,c), the regeneration of HMC<sup>+</sup> at potentials of the first wave is faster, leading to an enhancement of the anodic wave for HMC<sup>+</sup> oxidation at the expense of TPrA and the disappearance of the cathodic wave for HMC<sup>+</sup> reduction. The peak shapes of cyclic voltammograms show the effect of enhancement of TPrA concentration at potentials of the first wave.

Simulations were carried out with  $E^\circ = +0.55$  V for reaction 2. Various values of  $k_f$  for reaction 7 and  $E^\circ$  for reaction 4 were tried. The rapid deprotonation reaction, eq 5, and the other following reactions make the overall oxidation of TPrA irreversible. Although the  $E^\circ$  value for the oxidation of TPrA (or other alkylamines) to the radical cation has not been measured, one can obtain an estimate of this from measurements of various hindered species. Nelsen and Cunkle<sup>19</sup> showed that reversible voltammetry was observed with 9-neopentyl-9-azabicyclo[3.3.1]nonane and 9-(2-adamantyl)-9-azabicyclo[3.3.1]nonane with  $E^\circ$  values of about +0.9 V vs SCE. Although these trialkylamines are structurally different than TPrA, their  $E^\circ$  values should be

(19) Nelson, S. F.; Cunkle, G. T. *J. Org. Chem.* **1985**, *50*, 3701.

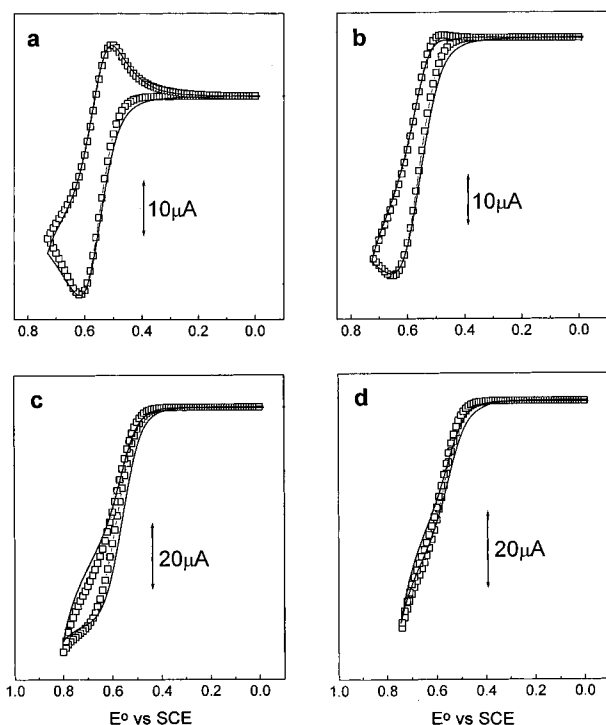


Figure 9. Effect of concentration on cyclic voltammograms at 0.2 V/s. Solid lines are experimental and open circles digital simulation. (a) 2.1 mM HMC<sup>+</sup> with 1.9 mM TPrA, (b) 1.7 mM HMC<sup>+</sup> with 5.3 mM TPrA, (c) 1.2 mM HMC<sup>+</sup> with 16.9 mM TPrA, and (d) 1.0 mM HMC<sup>+</sup> with 37.6 mM TPrA in MeCN; electrolyte, 0.1 M (TBA)PF<sub>6</sub>. Background was subtracted from the experimental data. Simulation parameters: eq 2,  $E^\circ = +0.55$  V vs SCE,  $\alpha = 0.5$ ,  $k_s = 1.8 \times 10^{-2}$  cm/s; eq 3,  $k_f =$  (a) 2500, (b) 2000, (c) 2000, and (d) 350 M<sup>-1</sup> s<sup>-1</sup>; eq 4,  $E^\circ = +0.805$  V vs SCE,  $\alpha = 0.5$ ,  $k_s = 3.0 \times 10^{-4}$  cm/s; eq 5,  $k_f = (1.0-2.8) \times 10^7$  M<sup>-1</sup> s<sup>-1</sup>; eq 8,  $k_f = 41$  s<sup>-1</sup>.

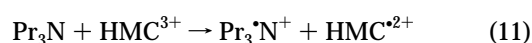
similar. Thus, simulations were undertaken with  $E^\circ$  values for reaction 4 at or above +0.805 V vs SCE. The fact that  $E^\circ$  for TPrA/TPrA<sup>+</sup> is more positive than that for HMC<sup>+</sup>/HMC<sup>2+</sup> implies that this scheme is an example of redox catalysis,<sup>20</sup> where the rapid irreversible reaction of TPrA<sup>+</sup> (deprotonation followed by reaction of the intermediate with HMC<sup>+</sup> and HMC<sup>2+</sup>) drives a thermodynamically unfavorable reaction. Best-fit simulation parameters are given in the captions of Figures 8 and 9. Because a number of kinetic parameters are involved in the overall reaction sequence, unambiguous values of the rate constants cannot be obtained; however, limits can be given. The rate constant for eq 3 is >2000 M<sup>-1</sup> s<sup>-1</sup>, while the lower limit for eq 5 is 10<sup>7</sup> M<sup>-1</sup> s<sup>-1</sup> (Figure 9). The rate constant of eq 7 had little effect upon the voltammetry response, even when set to near the mass transfer limit of 10<sup>10</sup> M<sup>-1</sup> s<sup>-1</sup>, since the overall contribution of this reaction to the removal of TPrA and regeneration of HMC<sup>+</sup> is small. To obtain a satisfactory fit to the observed cyclic voltammograms of HMC<sup>+</sup> in the absence and presence of TPrA, dimerization of HMC<sup>2+</sup> (reaction 8) had to be taken into consideration. The rate constant for eq 8 is around 41 s<sup>-1</sup>. At large  $v$ , e.g., 20 V/s (Figure 8d), the simulation was not affected by the dimerization reaction. To understand the mechanism with the TPrA coreactant in more detail, it will be necessary to understand the electrochemistry of TPrA and chemical reactions of the oxidation intermediates.

**ECL of HMC<sup>+</sup>/TPrA.** The ECL mechanism for HMC<sup>+</sup>/TPrA is similar to those of the Ru(bpy)<sub>3</sub><sup>3+</sup>/TPrA<sup>12,15,16</sup> and 9,10-diphe-

nylanthracenesulfonate (DPAS)/TPrA<sup>4d</sup> systems and proceeds via an oxidative-reduction mechanism. The oxidation of TPrA produces the strong reducing intermediate necessary to carry out ECL. From the voltammetry, oxidation of TPrA is believed to occur by the direct electrode reaction (eq 4) and in solution by reaction with HMC<sup>+</sup> (eq 3). The difference in the locations of the peak emission and peak current implies that the homogeneous oxidation of TPrA by HMC<sup>+</sup> may explain the initial rise in ECL, but the direct electrode oxidation of TPrA also produces the intermediate for light generation at more positive potentials, as implied in the reaction scheme of eqs 2–7.

In the HMC<sup>+</sup> system, the ECL emission observed is from the excited state HMC<sup>+\*</sup>, identical to that formed during photoexcitation. By analogy to the Ru(bpy)<sub>3</sub><sup>3+</sup>/TPrA system, the excited state is believed to be formed by reaction of the oxidized luminophore with the strongly reducing radical Pr<sub>2</sub>NC•HET. Unfortunately, no direct evidence exists for this mechanism for ECL or for the identity of the transient radical species. Indeed, the mechanism for the electrochemical oxidation of aliphatic amines in aprotic media is also largely unexplored.

When the concentration of either HMC<sup>+</sup> or TPrA was low, two ECL emission waves appeared during the potential sweep. The second ECL wave appeared at +1.2 V. This potential is very close to that for the oxidation of HMC<sup>2+</sup> to the trication. The ECL spectrum obtained by pulsing to this potential, however, only showed the emission in the near-IR region, indicating that the emitting state was HMC<sup>+</sup>. These reactions correspond to



so that oxidation at the more positive potentials would correspond to an additional source of the emission precursor, HMC<sup>2+</sup>.

In considering the energetics of an ECL system, one compares the standard potentials of the relevant half-reactions (yielding the free energy of the electron-transfer reaction) with the energy of the emitting state. The near-infrared ECL spectrum, with an emission peak at 800 nm for the HMC<sup>+</sup>/TPrA system, corresponds to a singlet energy of 1.6 eV. The total free energy available in the oxidative-reduction reaction is 1.65 eV, based on the difference between the half-reaction potentials of eqs 2 and 6. Thus, the energy available from the oxidative-reduction reaction is very close to that required for direct population of the singlet state (an S-route system). The potential for the oxidation of Pr<sub>2</sub>NC•HET assumed in the above calculation (-1.1 V vs SCE) has not been measured directly but has been taken to be similar in energy to that of Et<sub>2</sub>NC•HMe.<sup>21</sup>

## CONCLUSIONS

A new ECL reaction of a heptamethine cyanine dye containing seven methine carbon atoms has been observed in MeCN utilizing the coreactant tri-*n*-propylamine via an oxidative-reduction approach. The ECL emission appears at potentials where oxidation of HMC<sup>+</sup> and TPrA occurs, with no ECL observed when either or both are absent. When HMC<sup>+</sup> is oxidized in the presence of TPrA, a near-infrared ECL emission results, characteristic of HMC<sup>+</sup> fluorescence, and is the lowest-energy ECL reported to date.

(20) Andrieux, C. P.; Hapiot, P.; Saveant, J.-M. *Chem. Rev.* **1990**, *90*, 723.

(21) Wayner, D. D. M.; McPhee, D. J.; Griller, D. *J. Am. Chem. Soc.* **1988**, *110*, 132.

HMC<sup>+</sup>, which contains substituents within the pentamethine chain, exhibits reversible cyclic voltammetry. Radical persistence is attributed to electronic stabilization by alkyl substituents and to steric hindrance, leading to slow rates of dimerization. The heptamethine cyanine radical produced by the one-electron oxidation of a cationic dye exhibits an intense absorption band in the visible region. Digital simulation of the HMC<sup>+</sup>/TPrA system has allowed estimation of several homogeneous reactions and the standard potential for the oxidation of TPrA.

#### ACKNOWLEDGMENT

We thank Dr. Jeff D. Debad for helpful suggestions throughout this work and Ms. Hyeran Ihm for drawing the geometry of the molecule using molecular mechanics. Funding by the Robert A.

Welch Foundation, the Texas Advanced Research Program, and IGEN is gratefully acknowledged. L.S.K. thanks the Korea Science and Engineering Foundation for his support in the form of a Postdoctoral Fellowship.

#### SUPPORTING INFORMATION AVAILABLE

Molecular simulation of HMC<sup>+</sup> (1 page). See any current masthead page for ordering information and Internet access instructions.

Received for review May 5, 1997. Accepted July 26, 1997.<sup>⊗</sup>

AC9704570

---

<sup>⊗</sup> Abstract published in *Advance ACS Abstracts*, September 1, 1997.